



# CHORUS

This is the accepted manuscript made available via CHORUS. The article has been published as:

## Linear dichroism and the nature of charge order in underdoped cuprates

M. R. Norman

Phys. Rev. B **91**, 140505 — Published 21 April 2015

DOI: [10.1103/PhysRevB.91.140505](https://doi.org/10.1103/PhysRevB.91.140505)

# Linear dichroism and the nature of charge order in underdoped cuprates

M. R. Norman<sup>1</sup>

<sup>1</sup>*Materials Science Division, Argonne National Laboratory, Argonne, IL 60439, USA*

(Dated: April 3, 2015)

Recent experiments have addressed the nature of the charge order seen in underdoped cuprates. Here, I show that x-ray absorption and linear dichroism are excellent probes of such order. Ab-initio calculations reveal that a d-wave charge density wave order involving the oxygen ions is a much better description of the data than alternate models.

PACS numbers: 78.70.Dm, 75.25.Dk, 74.72.Kf

The observation of charge order in underdoped YBCO by NMR [1] followed by its observation by both soft [2] and hard [3] x-ray scattering, along with the probable role of the charge order in Fermi surface reconstruction [4], has been one of the most significant developments in the field of high temperature cuprate superconductivity in the past few years. Of particular note was the suggestion that the charge order was of a novel d-wave nature, involving charge modulations that are out of phase on the two oxygen ions in a given  $\text{CuO}_2$  unit [5]. Such a d-wave phasing relation has been inferred from Fourier transformed STM data [6] and is consistent as well with the azimuthal dependence of resonant x-ray scattering at the Cu  $L_3$  edge [7]. The latter work involved modeling the x-ray data as due to a spatial modulation of the energies of the copper 3d orbitals relative to the oxygen 2p ones [8].

Related to these measurements was a claim of seeing x-ray natural circular dichroism (XNCD) at the Cu K edge in underdoped Bi2212 [9]. An XNCD signal has been claimed as well in underdoped LBCO [10]. Although chiral charge order could cause an XNCD signal [11], a more natural explanation of the data is linear dichroism contamination, which is always present in circularly polarized beams [12]. This has been confirmed by recent measurements at the Cu K edge in Bi2212, where the expected azimuthal angular dependence of  $\cos(2\psi)$  for linear dichroism was seen in the “XNCD” signal [13].

Here, I show that in fact linear dichroism itself provides an exquisite probe of charge order in the cuprates if the ordering is one-dimensional in nature (stripes) as opposed to two-dimensional in nature (checkerboards) - in the latter case, there is no linear dichroism due to charge order. For calculational purposes, I consider  $\text{HgBa}_2\text{CuO}_{4+\delta}$  (Hg1201) since that material is tetragonal, meaning there is no structural linear dichroism to contend with. Calculations were performed with the multiple scattering Greens function code FDMNES [14] including spin-orbit interactions [15]. The simulations were done using local density atomic potentials (Hedin-Lundqvist exchange-correlation function) in a muffin tin approximation that considers multiple scattering of the photoelectron around the absorbing site [16, 17]. The

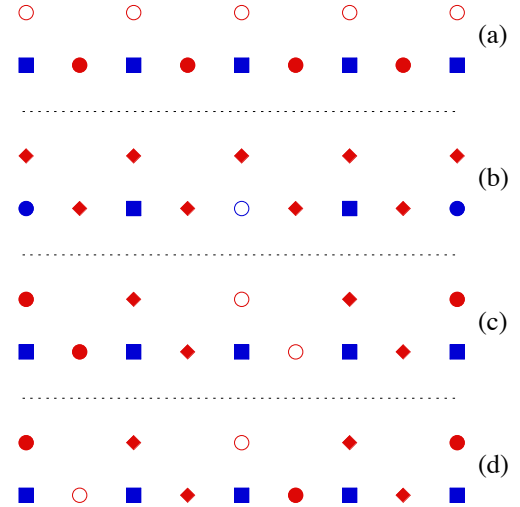


FIG. 1: (Color online) Charge modulation patterns assumed in this work for a charge ordering vector of 0.25 reciprocal lattice units. (a) is for nematic order, with blue squares the unmodulated copper sites, and filled (open) red circles oxygen sites with an excess (deficit) of 2p electrons. (b) is for a copper charge modulation, with blue squares the unmodulated copper sites, and filled (open) blue circles copper sites with an excess (deficit) of 3d electrons, with red diamonds the unmodulated oxygen sites. (c) is for an oxygen s-wave charge modulation, with blue squares the unmodulated copper sites, and filled (open) red circles oxygen sites with an excess (deficit) of 2p electrons, with unmodulated oxygen sites as red diamonds. (d) is for an oxygen d-wave charge modulation, with the same notation as in (c).

cluster radius is limited by the photoelectron lifetime [18]. Results shown here are in the energy range of the Cu  $L_2$  and  $L_3$  edges for a cluster radius of 5 Å (36 atoms surrounding each absorbing copper site), with calculations also performed at the Cu K and Cu  $L_1$  edges. Atom positions for Hg1201 were taken from Wagner *et al.* [19].

Fig. 1 shows the four ordering patterns assumed: (a) nematic order within a  $\text{CuO}_2$  unit (the two oxygen ions being out of phase), (b) charge modulation on the copper sites, (c) s-wave charge modulation on the oxygen sites (the two oxygen ions in each  $\text{CuO}_2$  unit are in phase), and

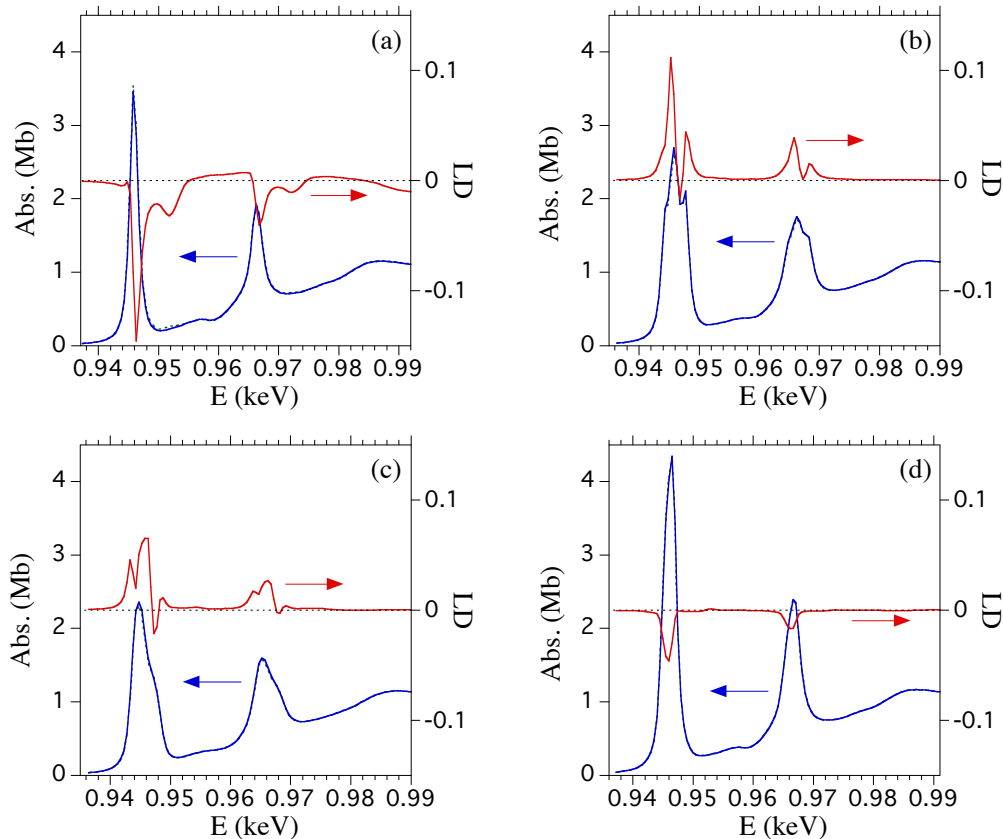


FIG. 2: (Color online) X-ray absorption in the energy range of the Cu  $L_3$  and  $L_2$  edges for a  $k$  vector along the  $c$ -axis for Hg1201. Two absorption curves are shown, one for the electric field vector along  $x$  (green dashed curve, left arrow), the other along  $y$  (blue solid curve, left arrow), noting that the two curves are almost identical. The prominent peaks are the  $L_3$  one near 946 eV and the  $L_2$  one near 966 eV. The linear dichroism (LD) is taken as the difference of the absorption for the electric field along  $y$  and that along  $x$  (red solid curve, right arrow), with the charge modulation wavevector along  $x$ . Each panel (a)-(d) corresponds to the modulations shown in Fig. 1, with a maximum charge modulation of  $\pm 0.05$  electrons.

(d)  $d$ -wave charge modulation on the oxygen sites (the two oxygen ions in each  $\text{CuO}_2$  unit are out of phase). To simplify the calculations, a charge ordering wavevector of 0.25 in reciprocal lattice units was assumed. Use of an incommensurate wavevector would lead to a smearing of the absorption features presented here.

In Fig. 2, results in the energy range of the Cu  $L_3$  and  $L_2$  edges are shown for the four cases illustrated in Fig. 1, assuming a maximum charge modulation of  $\pm 0.05$  electrons as assumed in earlier modeling [8]. Here, the x-ray  $k$  vector is directed along the  $c$  axis [20]. The absorption for nematic order (a) is similar to that without any charge modulation, except for the presence of a substantial dichroism near each absorption peak (almost 5% of the  $L_3$  absorption peak maximum). For copper charge modulation (b), one finds substantial broadening of the  $L_3$  and  $L_2$  absorption peaks due to splitting of the peaks from the fact that there are now three different copper sites (Fig. 1b). Similar broadening is also seen for the  $s$ -wave oxygen modulation case (c). For the  $d$ -wave modulation case (d), though, one finds  $L_3$  and  $L_2$  absorp-

tion peaks whose widths are only moderately larger than without charge order, with a significantly reduced linear dichroism (1% of the  $L_3$  absorption peak maximum).

In Fig. 3, results are shown analogous to Fig. 2, but for a maximum charge modulation of  $\pm 0.1$  electrons instead. For this increased value, one sees substantial splitting of the absorption peaks in all cases except for the case of nematic order. In addition, the linear dichroism signal is enhanced by roughly a factor of four. Although we do not show results for the Cu  $K$  and  $L_1$  edges, in those cases as well, a substantial dichroism exists. The energy profile of the absorption is also altered relative to that without charge order, and this is most pronounced for the case of an oxygen  $s$ -wave charge modulation.

The observed  $L_3$  absorption peaks of underdoped cuprates are actually quite narrow. For the case of Hg1201, the FWHM is around 1.2 eV with no sign of splitting of the peak [21]. If anything, even narrower peaks are seen in underdoped YBCO [2] and Bi2201 [22]. The simulation results presented here are actually broader than what is observed (1.7 eV for Fig. 2a, 4.3 eV

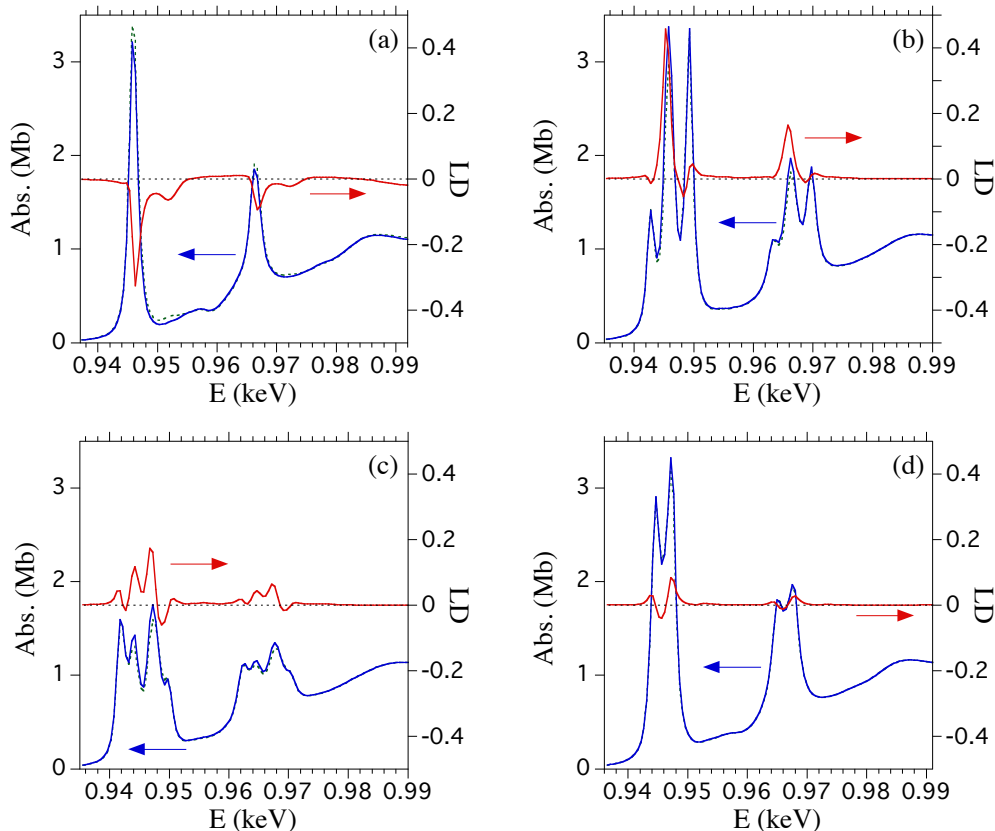


FIG. 3: (Color online) Same as Fig. 2, but for a maximum charge modulation of  $\pm 0.1$  electrons instead.

for Fig. 2b, 4.0 eV for Fig. 2c, and 2.5 eV for Fig. 2d). These widths could be reduced by reducing the assumed core hole broadening [18]. Regardless, the narrowness of the experimental peaks and the absence of any splitting is definitely inconsistent with either a charge modulation on the copper sites (Fig. 2b), or an s-wave modulation on the oxygen sites (Fig. 2c). As such, the results presented here are completely consistent with a d-wave pattern (Fig. 2d) as advocated in previous work [6, 7]. Further information could be obtained if the light spot imaged a single charge ordering domain, since for each charge modulation pattern, the linear dichroism has a unique energy profile. Regardless, even with domain averaging (or a checkerboard pattern), charge ordering should cause a broadening of the absorption peaks (Figs. 2 and 3), and this could be quantified by measuring the temperature dependence of the width of the  $L_3$  and  $L_2$  absorption peaks.

These results can easily be extended by looking at resonant x-ray scattering at the charge ordering wavevector. In addition, related results can be obtained in the case of spin ordering, where again, depending on the pattern (spins on the copper sites, or spins on the oxygen sites), one sees a significant difference in the dichroism [23]. The latter is particularly relevant, since resonant

x-ray scattering at the magnetic wavevector of underdoped cuprates is not possible at the Cu  $L_2$  and  $L_3$  edges because of kinematic constraints, making absorption the only ideal x-ray probe of the spin order [24].

In summary, x-ray absorption and linear dichroism are exquisite probes of charge order in cuprates, and can be used to determine the actual modulation pattern due to the site sensitivity of resonant x-rays. Similar considerations also apply to the incommensurate spin order seen for even more underdoped samples.

The author thanks Yves Joly and Sergio Di Matteo for several helpful discussions. This work was supported by the Materials Sciences and Engineering Division, Basic Energy Sciences, Office of Science, US DOE.

- 
- [1] T. Wu, H. Mayaffre, S. Kramer, M. Horvatic, C. Berthier, W. N. Hardy, R. Liang, D. A. Bonn and M.-H. Julien, *Nature* **477**, 191 (2011).
  - [2] G. Ghiringhelli, M. Le Tacon, M. Minola, S. Blanco-Canosa, C. Mazzoli, N. B. Brookes, G. M. De Luca, A. Frano, D. G. Hawthorn, F. He, T. Loew, M. Moretti Sala, D. C. Peets, M. Salluzzo, E. Schierle, R. Sutarto, G. A. Sawatzky, E. Weschke, B. Keimer and L. Braicovich, *Sci-*

- ence **337**, 821 (2012).
- [3] J. Chang, E. Blackburn, A. T. Holmes, N. B. Christensen, J. Larsen, J. Mesot, R. Liang, D. A. Bonn, W. N. Hardy, A. Watenphul, M. v. Zimmermann, E. M. Forgan and S. M. Hayden, *Nature Phys.* **8**, 871 (2012).
- [4] N. Harrison and S. E. Sebastian, *Phys. Rev. Lett.* **106**, 226402 (2011).
- [5] S. Sachdev and R. La Placa, *Phys. Rev. Lett.* **111**, 027202 (2013).
- [6] K. Fujita, M. H. Hamidian, S. D. Edkins, C. K. Kim, Y. Kohsaka, M. Azuma, M. Takano, H. Takagi, H. Eisaki, S.-i. Uchida, A. Allais, M. J. Lawler, E.-A. Kim, S. Sachdev and J. C. S. Davis, *Proc. Natl. Acad. Sci.* **111**, E3026 (2014).
- [7] R. Comin, R. Sutarto, F. He, E. da Silva Neto, L. Chauviere, A. Frano, R. Liang, W. N. Hardy, D. A. Bonn, Y. Yoshida, H. Eisaki, J. E. Hoffman, B. Keimer, G. A. Sawatzky and A. Damascelli, arXiv:1402.5415 (2014).
- [8] A. J. Achkar, F. He, R. Sutarto, J. Geck, H. Zhang, Y.-J. Kim and D. G. Hawthorn, *Phys. Rev. Lett.* **110**, 017001 (2013).
- [9] M. Kubota, K. Ono, Y. Oohara and H. Eisaki, *J. Phys. Soc. Japan* **75**, 053706 (2006).
- [10] Ruihua He, private communication.
- [11] M. R. Norman, *Phys. Rev. B* **87**, 180506(R) (2013).
- [12] S. Di Matteo and M. R. Norman, *Phys. Rev. B* **76**, 014510 (2007).
- [13] Young Lee, private communication.
- [14] Y. Joly, *Phys. Rev. B* **63**, 125120 (2001). The FDMNES program, along with extensive documentation, can be downloaded at <http://neel.cnrs.fr/spip.php?rubrique1007>
- [15] Y. Joly, O. Bunau, J. E. Lorenzo, R. M. Galera, S. Grenier and B. Thompson, *J. Phys.: Conf. Ser.* **190**, 012007 (2009).
- [16] C. R. Natoli, Ch. Brouder, Ph. Sainctavit, J. Goulon, Ch. Goulon-Ginet and A. Rogalev, *Eur. Phys. J. B* **4**, 1 (1998).
- [17] When constructing the potentials, it is assumed (for the unmodulated case) that the coppers are in a  $d^9 s^2$  configuration and the oxygens in a  $p^4 s^2$  configuration.
- [18] The results presented involve a convolution of the calculated spectrum with both a core hole (1.16 eV at the  $L_3$  edge, 1.66 eV at the  $L_2$  edge) and a photoelectron inverse lifetime, with the latter having a strong energy dependence (at high energies, 15 eV, with a midpoint value at 30 eV above the Fermi energy) [15]. Core hole widths tabulated in the FDMNES program are based on the x-ray literature [15].
- [19] J. L. Wagner, P. G. Radaelli, D. G. Hinks, J. D. Jorgensen, J. F. Mitchell, B. Dabrowski, G. S. Knapp and M. A. Beno, *Physica C* **210**, 447 (1993).
- [20] The calculated peaks are shifted in energy relative to experiment, though the energy separation of the  $L_3$  and  $L_2$  absorption peaks is the same.
- [21] W. Tabis, Y. Li, M. Le Tacon, L. Braicovich, A. Kreyssig, M. Minola, G. Della, E. Weschke, M. J. Veit, M. Ramazanoglu, A. I. Goldman, T. Schmitt, G. Ghiringhelli, N. Barisic, M. K. Chan, C. J. Dorow, G. Yu, X. Zhao, B. Keimer and M. Greven, *Nature Comm.* **5**:5875 (2014).
- [22] R. Comin, A. Frano, M. M. Yee, Y. Yoshida, H. Eisaki, E. Schierle, E. Weschke, R. Sutarto, F. He, A. Soumyanarayanan, Y. He, M. Le Tacon, I. S. Elfimov, J. E. Hoffman, G. A. Sawatzky, B. Keimer and A. Damascelli, *Science* **343**, 390 (2014).
- [23] Magnetic dichroism has a unique signature, with  $L_3$  and  $L_2$  peaks of opposite sign.
- [24] Resonant x-ray scattering at the magnetic wavevector is possible at the Cu K edge, but the effects are weak since only the orbital moment contribution on the copper sites can be probed.